

# Yield Strength of Transparent $\text{MgAl}_2\text{O}_4$ Nano-Ceramic at High Pressure and Temperature

Jie Zhang · Tiecheng Lu · Xianghui Chang ·  
Shengli Jiang · Nian Wei · Jianqi Qi

Received: 28 March 2010 / Accepted: 10 May 2010 / Published online: 23 May 2010  
© The Author(s) 2010. This article is published with open access at Springerlink.com

**Abstract** We report here experimental results of yield strength and stress relaxation measurements of transparent  $\text{MgAl}_2\text{O}_4$  nano-ceramics at high pressure and temperature. During compression at ambient temperature, the differential strain deduced from peak broadening increased significantly with pressure up to 2 GPa, with no clear indication of strain saturation. However, by then, warming the sample above 400°C under 4 GPa, stress relaxation was obviously observed, and all subsequent plastic deformation cycles are characterized again by peak broadening. Our results reveal a remarkable reduction in yield strength as the sintering temperature increases from 400 to 900°C. The low temperature for the onset of stress relaxation has attracted attention regarding the performance of transparent  $\text{MgAl}_2\text{O}_4$  nano-ceramics as an engineering material.

**Keywords** Transparent  $\text{MgAl}_2\text{O}_4$  nano-ceramics · High pressure/temperature · Differential strain · Yield strength · Stress relaxation

## Introduction

It is generally believed that nano-grained ceramics have their unique mechanical characteristics that are not commonly found in their coarse-grained counterparts [1]. Strength is an important aspect of material for mechanical and particular applications under loading and static pressure. In some case, it is desirable to optimize strength to improve performance. One important example is ceramic armor [2]. Transparent  $\text{MgAl}_2\text{O}_4$  ceramic has received considerable attention and has been widely studied [3–6] because of its high melting point, good mechanical strength, high resistance against chemical attack, and extraordinary optical properties [7–11]. Presently, extensive work has been performed in studying the fabrication [12, 13], micro-morphology [14, 15] and transparent mechanism [16] of transparent  $\text{MgAl}_2\text{O}_4$  nano-ceramic. However, there is limited research on investigating one of the fundamental parameters of transparent  $\text{MgAl}_2\text{O}_4$  nano-ceramic the yield strength at high pressure and temperature. The aim of this work is to study the yield strength of transparent  $\text{MgAl}_2\text{O}_4$  nano-ceramic at pressure up to 5 GPa and temperature up to 900°C through the analysis of the shape of X-ray diffraction lines.

## Experiment and Discussion

We carried out X-ray diffraction experiments on transparent  $\text{MgAl}_2\text{O}_4$  nano-ceramic using X-ray ( $\text{CuK}\alpha$ ) diffractometer (Model DX-2500). The nano- $\text{MgAl}_2\text{O}_4$  powder, with a median particle size of 30 nm, was prepared by a low-cost melted-salt technique [12]. Two separated layers of nano- $\text{MgAl}_2\text{O}_4$  and NaCl cylinder were loaded inside a cubic pyrophyllite cell, which is a pressure-transmitting

J. Zhang · T. Lu (✉) · X. Chang · S. Jiang · N. Wei · J. Qi  
Department of Physics and Key Laboratory for Radiation  
Physics and Technology of Ministry of Education, Sichuan  
University, 610064 Chengdu, People's Republic of China  
e-mail: lutiecheng@scu.edu.cn

J. Zhang  
e-mail: zhjie126@126.com

T. Lu  
International Center for Material Physics, Chinese Academy of  
Sciences, 110015 Shenyang, People's Republic of China

medium, and assembled to the press-standing piece with other modules including a carbon heater. The temperature was measured by a Nichrome-NiSi thermocouple, which was passed through the press-standing piece in advance of calibrating the sintering temperature. The samples were compressed from 1 to 5 GPa at room temperature and then heated from 300 to 900°C under 4 GPa.

The observed diffraction patterns plotted in Fig. 1 are selected to present peak profile changes of samples at various P–T conditions. During the compression from ambient to 2 GPa at room temperature, the samples' peaks broaden asymmetrically, with a much more severe broadening on the large angular dispersive ( $2\theta$ ) side of the peak, as shown in the bottom two curves of Fig. 1. The results reveal that the applied pressure only affects the bridge parts of the grains. Meanwhile, the generated stress is not enough to cause any yielding at this stage. As pressure increases gradually, differential strain and small grain size are two major causes of peaks broadening [17]. During heating at constant pressure (4 GPa), the overall peaks remained almost unchanged up to 400°C. The peaks are significantly sharp and become more symmetric at temperatures above 400°C, which is a clear proof of stress relaxation accompanied by stress redistribution over the entire sample (Fig. 1, the top two curves). It is interesting to note that the peaks shift to lower  $2\theta$ . This shift is apparently due to the effect of heating. The profile of the observed diffraction peaks is a convolution of integrated effect of instrument response, grain size, and differential strain ( $\varepsilon$ ) because of stress heterogeneity, lattice deformation, and dislocation density at high pressure and temperature [18]. We express that the observed full width at half maximum (FWHM) can be denoted as  $\Delta d_{\text{obs}}$ . According to the classic Williamson-Hall method and its subsequent variations [19, 20], the differential strain ( $\varepsilon$ ) of samples is defined as

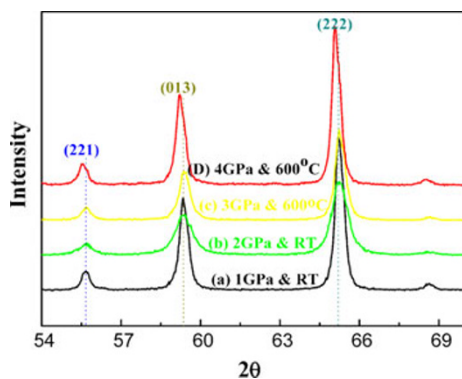


**Fig. 1** (221), (013) and (222) diffraction lines of  $\text{MgAl}_2\text{O}_4$  at selected pressure and temperature conditions: **a** 1 GPa, room temperature, **b** 2 GPa, room temperature, **c** 3 GPa, 600°C and **d** 4 GPa, 600°C

$$\Delta d_{\text{obs}}^2 = \Delta d_{\text{ins}}^2 + \Delta d_{\text{size}}^2 + \varepsilon^2 d^2(P, T). \quad (1)$$

Here,  $\Delta d_{\text{ins}}$  is the peak width at a stress-free state and  $d(P, T)$  is the  $d$  spacing of a given lattice plane. In our calculations, we subtract the instrument resolution, but we cannot disjoin the various contributions to the peak width changes. Therefore, we determined the strain by the ratio of the peak width to the peak position according to  $d$  spacing [20, 21]

$$\varepsilon = \Delta d_{\varepsilon}/d = \sqrt{\Delta d_{\text{obs}}^2 - \Delta d_{\text{ins}}^2}/d(P, T) \quad (2)$$

Such defined strain  $\varepsilon$  can be derived from the slope of  $\Delta d_{\varepsilon}$  versus  $d(P, T)$  plot (Fig. 2), which is an image of the complex contributions to the overall peak width changes. Figure 2 shows the significant slope changes associated with six selected pressure–temperature conditions. With increasing pressure from 1 to 5 GPa at room temperature, the derived differential strains increased dramatically, such as  $\varepsilon = 0.0766 \times 10^{-2}$  at  $P = 1$  GPa and  $\varepsilon = 0.4466 \times 10^{-2}$  at  $P = 5$  GPa, respectively. The strains described here are derived from the peak broadening, which are different from the regular strains [21]. As temperature (above 400°C) is increased at constant pressure (4 GPa), there is a rapid reduction in the differential strain, which is probably caused by thermally induced strain relaxation because of a small increase in the internal cell pressure.

The grain size, especially when it goes down to nanometer, contributes significantly to the diffraction line broadening [22]. Hence, we investigated details about the dependence of the differential stress as a function of pressure, and temperature could be revealed by introducing the grain size in the same plot.

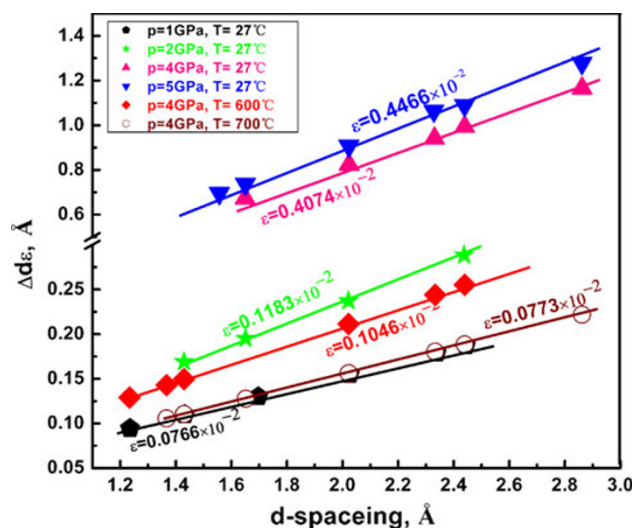
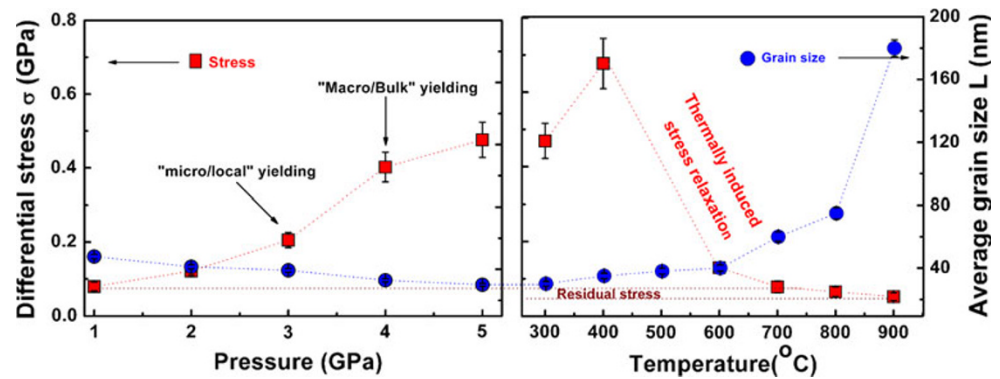


**Fig. 2** The plot of  $\Delta d_{\varepsilon}$  versus  $d(P, T)$  according to Eq. (2). The slopes of straight lines provide differential strain information for the sample

**Fig. 3** The yield strength and average grain size as function of pressure (*left panel*) and temperature (*right panel*). The lines are meant to guide the eye only



The strains have been derived for sample and for all high pressure/temperature observed. The strains are then converted to stresses through a stress–strain relationship of  $\sigma = E\varepsilon$  where  $E$  is Young’s modulus [23]. We obtain the Young’s modulus values of 294 GPa for samples by nano-indentation experiment. The calculated differential stresses and average grain size at various pressure and temperature conditions as blank-squares and solid-circles plots, respectively (Fig. 3). As pressure increases, we observed two obvious yield points for samples, one at  $P = 3$  GPa in the elastic deformation stage and the other at  $P = 4$  GPa. We think that the first yield represents “micro/local” due to the grain-to-grain contacts and thus local plastic deformation because of high stress concentration, and the second yield represents the onset of “macro/bulk” plastic deformation of the entire sample. Moreover, there is a slight addition of differential stress after the yielding when pressure changes from 4 to 5 GPa. Meanwhile, the diffraction peak widths do not vary as much after the entire sample yields. Our experiment results show that the dislocation density of the sample reaches certain saturation [24].

We studied temperature effects on the yield strength of sample at 4 GPa. As temperature is increased to 400°C at constant pressure (Fig. 3, right), there is a dramatically addition in the differential stress, which can be explained on the basis of our early discussion [16]. Above 400°C, the stress drops drastically with heating to 700°C due to thermally induced stress relaxation. On the other hand, there is a slight negative slope in the differential stress with the temperature above 700°C, which indicates that the sample gradually approaches a stress-free state. The plot still shows grain size effects on the sample at this high pressure and temperature (Fig. 3, blue-solid-circles). Figure 3, left reveals that there is no apparent grain growth at different high pressure. However, as temperature is increased to 700°C (Fig. 3, right), there is a fast grain growth. The results show that both stress relaxation and grain growth occur simultaneously during the temperature increases. To further take this interpretation, Palosz [25] and Gleiter [26] developed a model for nano-crystals, which are generally

viewed to consist of two structurally distinct components, a crystalline core and a surface layer. The differential strain may also be due to the difference in elastic properties between these two components [25]. As grain size gradually grows with increasing temperature, the distinction between these two components is expected to diminish, which may also explain the more rapid decrease in the strength with increasing temperature.

## Conclusion

In summary, yield strength is an important constitutive property of materials to define the onset of plastic deformation. And we have shown the yield strength of transparent  $\text{MgAl}_2\text{O}_4$  nano-ceramic as a function of high pressure/temperature. The excellent data reveal that the differential stress in nano-ceramic decreases as defects decrease during temperature increase, while grain growth further sharpens the diffraction peak. More importantly, the low temperature (400°C) for the onset of stress relaxation has attracted attention regarding the performance of transparent  $\text{MgAl}_2\text{O}_4$  nano-ceramics as an engineering material.

**Acknowledgments** This work was supported by NSFC of P. R. China under grant No 50272040, Fok Ying Tong Education Foundation under grant No 91046, Youth Foundation of Science and Technology of Sichuan Province under grant No 03ZQ026-03, NSFC of P. R. China under grant No 50742046 and NSFC of P. R. China under grant No 50872083.

**Open Access** This article is distributed under the terms of the Creative Commons Attribution Noncommercial License which permits any noncommercial use, distribution, and reproduction in any medium, provided the original author(s) and source are credited.

## References

1. B. Jiang, G.J. Weng, *Inter. J. Plastic.* **20**, 2007 (2004)
2. T.J. Vogler, L.C. Chhabildas, *Inter. J. Impact Eng.* **33**, 812 (2006)

3. R.J. Bratton, J. Am. Ceram. Soc. **57**, 283 (1974)
4. C.-T. Wang, L.-S. Lin, S.-J. Yang, J. Am. Ceram. Soc. **75**, 2240 (1992)
5. M. Shimada, T. Endo, T. Sato, Mat. Lett. **28**, 413 (1996)
6. C.-J. Ting, H.-T. Lu, Acta Mater. **47**, 817 (1999)
7. J.J. Swab, J.C. Lasalvia, G.A. Gilde, P.J. Patel, M.J. Motyka, Ceram. Eng. Sci. Proc. **20**, 79 (1999)
8. M.C.L. Patterson, J.E. Caiazza, G. Gilde, D.W. Roy, Ceram. Eng. Sci. Proc. **21**, 423 (2000)
9. M.C.L. Patterson, J.E. Caiazza, D.W. Roy, Proc. SPIE. **4102**, 59 (2000)
10. A.F. Dericioglu, Y. Kagawa, J. Eur. Ceram. Soc. **15**, 249 (1995)
11. J.G. Li, T. Ikegami, J.H. Lee, T. Mori, Y. Yajima, J. Eur. Ceram. Soc. **21**, 139 (2001)
12. T.C. Lu, X.H. Chang, J.Q. Qi, X.J. Luo, Appl. Phys. Lett. **88**, 213120 (2006)
13. H.J. Zhang, X.L. Jia, Z.J. Liu, Z.Z. Li, Mater. Lett. **58**, 1625 (2004)
14. X.H. Chang, T.C. Lu, J.Q. Qi, X.J. Luo, Key Eng. Mater. **336–338**, 2308 (2007)
15. J.F. Al-Sharab, F. Cosandey, J. Am. Ceram. Soc. **89**, 2279 (2006)
16. J. Zhang, T.C. Lu, X.H. Chang, N. Wei, W. Xu, J. Phys. D Appl. Phys. **42**, 052002 (2009)
17. F.W. Willets Brit, J. Appl. Phys. **16**, 323 (1965)
18. L. Gerward, S. Morup, J. Appl. Phys. **47**, 822 (1976)
19. G.K. Williamson, W.H. Hall, Acta Metall. **1**, 22 (1953)
20. Y.S. Zhao, J.Z. Zhang, J. Appl. Cryst. **41**, 1095 (2008)
21. Y.J. Wang, J.Z. Zhang, Y.S. Zhao, Nano Lett. **7**, 3196 (2007)
22. H.P. Klug, L.E. Alexander, *X-ray Diffraction Procedures for polycrystalline and Amorphous Materials* (John Wiley & Sons, New York, 1974)
23. D.J. Weidner, Y. Wang, M.T. Vaughan, Science **266**, 419 (1994)
24. Y.S. Zhao, J.Z. Zhang, B. Clausen, T.D. Shen, G.T. Gray III, L.P. Wang, Nano Lett. **7**, 426 (2007)
25. B. Paloze, J. Phys. Condens. Mater. **15**, 1 (2003)
26. H. Gleiter, Prog. Mater. Sci. **33**, 223 (1989)